J Therm Anal Calorim (2011) 104:901–907
DOI 10.1007/s10973-011-1490-0

Nucleation kinetics of a new nonlinear optical crystal

Urea–thiourea zinc chloride

S. C. Mojumdar · G. Madhurambal · M. Mariappan · B. Ravindran

CTAS2010 Conference Special Chapter

Abstract The induction period of various proportion of urea–thiourea zinc chloride crystal in water has been measured experimentally using the visual observation method. The induction period, which is inversely proportional to the nucleation rate, has been used to estimate the interfacial tension between the urea–thiourea zinc chloride and water; hence, the nucleation parameters like critical radius (r^*), number of molecules in the radius (r^*) and Gibbs free energy change for the formation of a critical nucleus (ΔG^*) have been calculated.

Keywords Solubility · Induction period · Interfacial tension · Critical radius · Critical nucleus

S. C. Mojumdar (✉)
Department of Chemical and Biochemical Engineering, The University of Western Ontario, London, Ontario N6A 5B9, Canada
e-mail: scmojumdar@yahoo.com

S. C. Mojumdar
Department of Chemical Technologies and Environment, Faculty of Industrial Technologies, Trenčín University, 020 32 Púchov, Slovakia

G. Madhurambal
A D M College for Women, Nagapattinam 611001, Tamil Nadu, India

M. Mariappan
EGS Pillay Engineering College, Nagapattinam 611002, Tamil Nadu, India

B. Ravindran
Department of Physics, EGS Pillay Engineering College, Nagapattinam, Tamil Nadu, India

Introduction

Nonlinear optical (NLO) materials showing second harmonic generation (SHG) have been in demand over the last few decades due to technological importance in the fields of optical communication, signal processing, and instrumentation [1–4]. Amongst them, the nonlinearity of urea is comparable with that of another important commercial NLO material potassium dihydrogen phosphate (KDP) [5, 6]. Until the last decade the materials explored for NLO application were mostly inorganic. However, it was realized that inorganic materials have lower probability for a centric structures and consequently scientists focused their attention to organic materials. Urea crystals attract the attention of both theoreticians and experimentalists due to the NLO piezoelectric properties. Urea is representative of one class of materials, which are applicable to photonics and reference material in the DMOS (diffusive mixing of organic solution) experiment in microgravity carried out by NASA [7]. They are potentially useful materials for frequency doubling of near IR laser radiation single crystals of the material which have very high laser damage threshold [8]. Nonlinear optics is playing a major role in emerging photonic and optoelectronic technologies. New NLO frequency conversion materials have a significant impact on laser technology and optical data storage [9]. Thiourea is an interesting inorganic matrix modifier due to its large dipole moment and its ability to form an extensive network of hydrogen bonds. It belongs to the orthorhombic crystal system. However, most of the thiourea complexes crystallize in centro symmetric form at room temperature and do not show SHG. Only a few of thiourea complexes viz, zinc thiourea sulphate [10], cadmium thiourea acetate [11], bis thiourea cadmium chloride [12], allyl thiourea mercury bromide [13], thio semicarbazide cadmium bromide [10] and

bismuth thiourea bromide [14] crystallize in non centro symmetric structure and show SHG. The search for new and efficient NLO materials has resulted in the development of a new class of materials called semiorganic crystals [15]. Thermodynamic/thermal, microscopic, optical and spectral studies are very useful techniques for materials characterization. Therefore, it is not surprising that many authors have applied these techniques for various materials characterization [16–29]. Motivated by these considerations urea–thiourea zinc chloride (UTZC) single crystals were synthesized, grown by slow evaporation technique at room temperature and studied by thermodynamic, microscopy, optical analysis and solubility test.

Experimental procedure

There are several methods of measuring the induction period depending on the solubility of materials. In this study, the visual observation method was followed. Solutions at different saturation values were prepared. The experimental set up consists of small cells of identical volume placed in a constant temperature bath, and the temperature was controlled to an accuracy of plus or minus 0.01 °C. A sensitive thermometer was inserted into this cell. As the temperature of solution reaches the temperature of the bath, the time was recorded until the nucleation starts and a visible speck appears. The time period that elapses between achievement of super saturation and appearance of visible nuclei is taken the induction period (τ). Several trial runs were performed to minimise the error. From the results obtained, a plot of $\ln\tau$ against $1/(\ln S)^2$ is drawn. From the slope of the curves, interfacial tension was calculated using the Eq. 1

$$\ln\tau = \ln A + 16\pi\gamma^3 V^2 N/3RT(\ln S)^2 \quad (1)$$

where A is a constant related to the pre-exponential factor of the nucleation rate expression, V is the molar volume, N is the Avagadro number, S is solubility and R is the gas constant. The factor $16\pi/3$ in the above equation refers to the spherical nuclei. The interfacial tension between the urea–thiourea mixed crystal nucleus and water was calculated by measuring the slope value of the curve obtained at these three different temperatures. The values are given in Table 1. According to the classical homogeneous nucleation theory, the free energy required to form a nucleus is given by

$$\Delta G = (4/3)\pi r^3 \Delta G_v + 4\pi r^2 \gamma \quad (2)$$

where ΔG_v is the energy change per unit volume, r is the radius of the nucleus. At the critical state, the free energy of formation obeys the condition that $d(\Delta G)/dr = 0$. Hence

Table 1 Effect of temperature on solubility and interfacial tension in various proportions of UTZC

Proportions	Solvent	Temperature/K	Solubility/g/100 mL	Interfacial tension (v)/mJ/m^2
0.1	Water	303	86.9	3.9764
		305	119.5	4.1712
		307	154.2	4.3266
0.25	Water	303	86.1	3.9845
		305	91.6	4.0298
		307	97.2	4.0728
0.5	Water	303	85.0	4.0045
		305	90.4	4.0491
		307	96.2	4.0941
0.66	Water	303	38.5	3.3722
		305	44.1	3.4584
		307	50.3	3.5412
0.75	Water	303	33.3	3.2950
		305	39.1	3.3978
		307	44.8	3.4853
0.9	Water	303	26.2	3.1618
		305	32.1	3.2943
		307	38.3	3.4094

the radius of the critical nucleus is expressed as $r^* = -2\gamma/\Delta G_v$, where $\Delta G_v = -kT\ln S/v$, where v is molecular volume.

Hence $r^* = 2v\gamma/kT\ln S$. The critical free energy is given by $\Delta G^* = 16\pi\gamma^3 v^2/\Delta G v^2$. The number of molecules in the critical nucleus is expressed as $i^* = 4\pi(r^*)^3/3v$. Using the interfacial tension, calculated from the slope of the curves obtained experimentally the radius of the critical nuclei (r^*), the free energy change for the formation of a critical nucleus (ΔG^*) and number of molecules in the critical nucleus (i^*) were calculated at three different temperatures and presented in Table 2. It was noted that with the increase in super saturation, the free energy change decreases (ΔG^*) with radius (r^*). This favours the easy formation of nucleation in 0.5 urea–thiourea zinc chloride crystal when compared to other proportions.

Solubility

The literature survey indicates the organic urea, thiourea salts as NLO materials. The salts used for the experiments are Analar Merck grade. The salts were recrystallized using water. It is essential to increase purity to a respectable level before proceeding further. Considerably recrystallization will produce material which is pure for crystal growth. Urea, thiourea salts are recrystallized with distilled water. Saturated solutions of urea and thiourea were prepared at 40 °C. The solutions were filtered to avoid any insoluble

Table 2 Effect of temperature on lnτ and $1/(\ln S)^2$ in various proportions of UTZC

Proportions	Solvent	Temperature/K	lnτ	$1/(\ln S)^2$
0.1	Water	303	10.6995	0.0502
		305	10.6897	0.0437
		307	10.6829	0.0394
0.25	Water	303	10.6753	0.0504
		305	10.6666	0.0490
		307	10.6575	0.0477
0.5	Water	303	10.6551	0.0507
		305	10.6461	0.0493
		307	10.6368	0.0480
0.66	Water	303	9.2899	0.0750
		305	9.2534	0.0698
		307	9.2183	0.0651
0.75	Water	303	9.3233	0.0814
		305	9.2864	0.0744
		307	9.2568	0.0692
0.9	Water	303	9.3644	0.0938
		305	9.3259	0.0831
		307	9.3004	0.0752

impurities using heated apparatus to prevent nucleation. The solutions were cooled down to room temperature to obtain maximum yield. The resulted crystals were recrystallized further. The fine powdered crystals were filtered off by suction and were air dried at room temperature. The purity was then checked by determining melting point.

Doubly distilled water was used in all the experiments. First of all the solubility of the salts were determined. The experimental procedure adopted was as follows.

The saturated urea, thiourea, and solutions 1 to 6 are prepared individually. Then, the empty weight of silica crucible was weighed. 5 mL of saturated solution was taken in a crucible and it was also weighted. From this the solubility of urea in 100 mL of water was found as 108.09 g and that of thiourea was 10.58 g. Similarly the solubility of 0.1, 0.25, 0.5, 0.66, 0.75 and 0.9 urea–thiourea zinc chloride crystals was tabulated in Table 1. It was observed that the salt thiourea is less soluble so the proportions of the crystals were expressed in terms of less soluble salt. From the Fig. 1, it is clearly shown that the solubility decreases with the increase in thiourea proportions.

Nucleation kinetics

Solution 1: (0.1UTZC-series1) 1 g of urea, 9 g of thiourea and 5 g of zinc chloride was dissolved in 27 mL of distilled water (Series1).

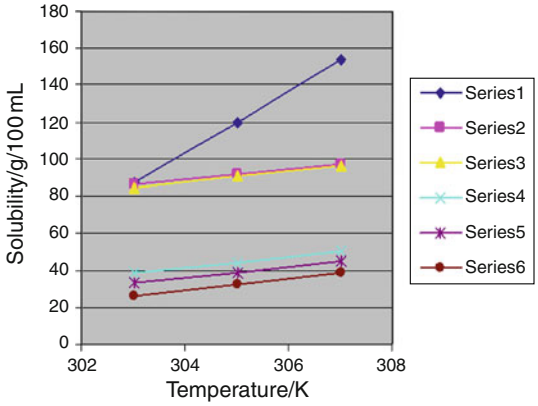

Fig. 1 Solubility of various proportions of UTZC in water

Solution 2: (0.25UTZC-series2) 2.5 g of urea, 7.5 g of thiourea and 5 g of zinc chloride was dissolved in 25 mL of distilled water (Series2).

Solution 3: (0.5UTZC-series3) 5 g each of urea, thiourea and zinc chloride was dissolved in 35 mL of distilled water (Series3).

Solution 4: (0.66UTZC-series4) 6.6 g of urea, 3.4 g of thiourea and 5 g of zinc chloride was dissolved in 45 mL of distilled water (Series4).

Solution 5: (0.75UTZC-series5) 7.5 g of urea, 2.5 g of thiourea and 5 g of zinc chloride was dissolved in 58 mL of distilled water (Series5).

Solution 6: (0.9UTZC-series6) 9 g of urea, 1 g of thiourea and 5 g of zinc chloride was dissolved in 70 mL of distilled water (Series6).

The crystal growth solutions should be in equilibrium at room temperature (303 K) and should not contain any spurious nuclei. The procedure adopted can be explained by taking solution 1, a saturated solution at a temperature slightly higher than initially required was prepared and filtered through a hot sintered glass flask. The solution was stirred using magnetic stirrer for about 6 h. The undissolved material collected at the bottom of the same flask and the clean solution was transferred to another flask and it is slightly heated above 5 K so that the undissolved material gets completely dissolved. After dissolving, filtration of the solution which plays a vital role (i.e. chemical purity of the solution) during growth is preformed.

The filtration of the solution was preformed with a Buckner funnel and filtration assembly. A filter paper of the size of Buckner funnel is taken and placed over its perforated disc. It is then fitted in a filtration flask connected to suction pump. The rate of filtration through conical flask considerably increased using a perforated filter paper. Thus, purified solution has prepared. Whilst transferring

the solution, temperature of the growth chamber was brought down to 2 K above the saturation temperature (32 °C); doing so the seed crystal may dissolve slightly as the solution was under saturated. Since periphery of the crystals dissolve in this case clear and clean, seed will be remaining. The temperature of the solution was adjusted to saturation temperature (303 K), the seed dissolution stops. After that the flask was covered with polyethylene sheets, in which small holes were bored to allow slow evaporation. Similar procedure was adopted for Solution 2, 3, 4, 5 and 6. As the temperature of the bath, the time was recorded until the nucleation starts, and appearance of visible nuclei was taken as the induction period. It was observed that for all the mixed crystals, the induction period decreased of the solutions from 0.1 to 0.5 and then slightly increased of the solutions from 0.66 to 0.9.

Results and discussion

Solubility and nucleation kinetics of UTZC

In varying proportions (0.1, 0.25, 0.5, 0.66, 0.75 and 0.9) of UTZC, a fixed weight of zinc chloride (5 g) was added as dopant and prepared the saturated solution with various solvents. Growth rate and characterization studies were performed for these solutions. The solubility of various proportions of UTZC was determined as a function of temperature, and the results are shown in Fig. 1. The solubility of various proportions of UTZC crystal decreases with increase in proportions of thiourea. Effect of temperature on $\ln\tau$ and $1/(\ln S)^2$ in various proportions of UTZC are summarized in Table 2. Figure 2 shows the induction period as function of various temperatures (in our experiments, the induction period τ was measured by the most commonly used method visual observation method). In this study, the nucleation kinetics of UTZC from various proportions has been carried out to calculate the interfacial tension between the crystal and water. The interfacial tension can be calculated from the graph drawn between $\ln\tau$ and $1/(\ln S)^2$. The measured interfacial tensions vary from 3.1618 to 4.3266 mJ/m^2. The value of interfacial tension of UTZC in 0.1, 0.25 and 0.5 proportions has much higher value compared to 0.66, 0.75 and 0.9. Based on nucleation theory, interfacial tension was calculated. The free energy change as a function of temperature is given in Fig. 3. It is clear that the free energy exponentially decreases with increase in temperature. The values of critical radius, number of molecules in the critical nucleus were decreased, and small values of free energy of activation in 0.9 proportion of UTZC when compared to all other proportions predict the easy formation of nucleation in water (Table 3).

Morphological studies

From the photographs shown in Figs. 4, 5, 6, 7, 8 and 9, it was identified that due to addition of the dopant zinc chloride the morphologies in all proportions of urea–thiourea mixed crystal (UTMC) are completely changed. This may be due to the formation of urea–thiourea zinc chloride, and this is further confirmed by UV and FTIR spectral studies. The laser activity of the UTZC is found to be higher when compared with UTMC crystal by higher green light emission by Wurtz powder technique.

SHG efficiency

The optical absorption of the crystalline sample was recorded using Kurtz powder technique. The NLO property

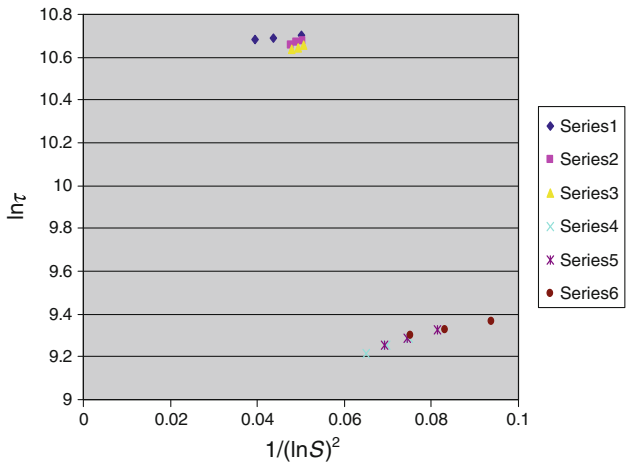

Fig. 2 A plot of $\ln\tau$ versus $1/(\ln S)^2$ of UTZC in water

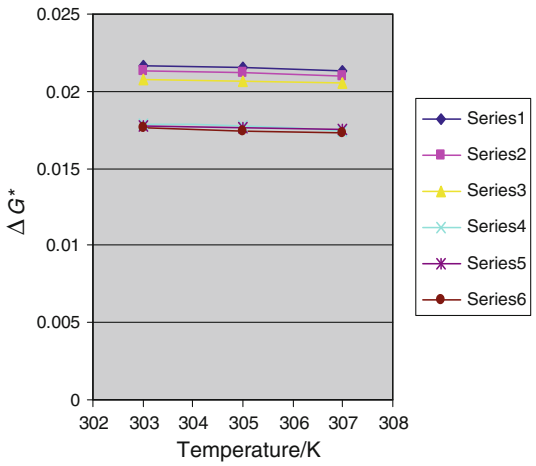

Fig. 3 Relation between the free energy change (ΔG^*) and temperature for UTZC

Table 3 Nucleation parameters of urea–thiourea zinc chloride in water

P	$r^*/10^{-10}$ m	ΔG^*/mJ/m^2 at 303 K	i^*	$r^*/10^{-10}$ m	ΔG^*/mJ/m^2 at 305 K	i^*	$r^*/10^{-10}$ m	ΔG^*/mJ/m^2 at 307 K	i^*
0.1	3.9182	0.0217	27.3661	3.8114	0.0215	25.1888	3.7288	0.0213	23.5863
0.25	3.9098	0.0213	27.3692	3.8734	0.0212	26.6119	3.8387	0.0210	25.9031
0.5	3.8964	0.0208	27.3899	3.8605	0.0207	26.6397	3.8250	0.0205	25.9116
0.66	3.9646	0.0179	29.0594	3.8945	0.0177	27.5451	3.8288	0.0174	26.1744
0.75	4.0179	0.0178	30.3711	3.9359	0.0176	28.5489	3.8674	0.0175	27.0839
0.9	4.1108	0.0176	32.7455	4.0146	0.0174	30.4980	3.9194	0.0173	28.3812

P Proportions

Fig. 4 0.1UTZC

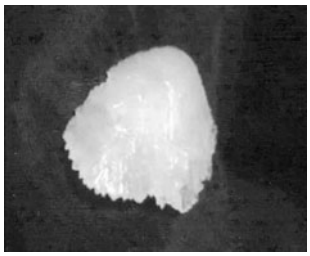

Fig. 5 0.25UTZC

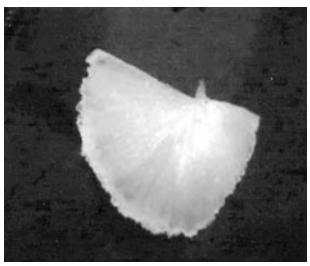

Fig. 6 0.5UTZC

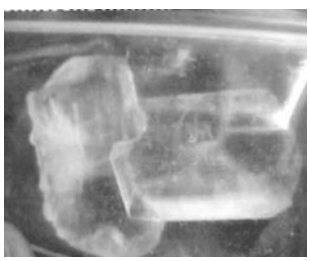

Fig. 7 0.66UTZC

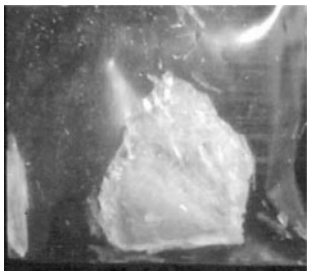

Fig. 8 0.75UTZC

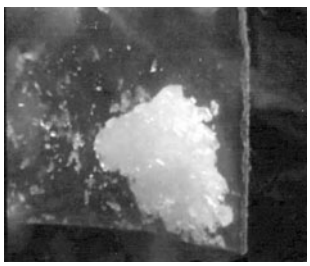

Fig. 9 0.9UTZC

of various proportions of UTZC crystal was confirmed by shining Nd:YAG laser ($\lambda = 1046$ nm) on thin plate of the grown crystal. It is observed that green light is coming out of the crystal. The crystals are ground into powder and densely packed between two transparent glass slides. An Nd:YAG laser beam of wavelength 1046 nm was made to fall normally on the sample cell. The transmitted fundamental wave was absorbed by a copper sulphate solution, and second harmonic signal was detected by a photo multiplier tube and displayed on a storage oscilloscope. A different proportion of UTZC crystals, powdered to the identical size, were used as reference material in the SHG measurement. Although many materials have been identified that have higher molecular non-linearities, the attainment of second order effects requires favourite alignment of the molecule within the crystal structure. The efficient SHG demands specific molecular alignment of the crystal

to be achieved facilitating non-linearity in the presence of dopant. It has been reported that the SHG can be greatly enhanced by altering the molecular alignment through inclusion complexation.

Scanning electron microscopic (SEM) studies of UTZC

The SEM images are produced by scanning the sample with a focused electron beam and detecting the secondary and back scattered electrons from the conventional SEM image. The main advantages of SEM are due to much larger magnification possibility since electron wavelengths are much smaller than photon wavelengths and the depth of the field is much larger. The electron wavelength λ_e depends on the electron velocity V_e or the accelerating voltage V as

$$\lambda_e = h/mV_e = 12.2/\sqrt{V}$$

The wavelength is 0.12 A° for $V = 10{,}000\ V$ which is significantly less than the 4,000 to 7,000 A° wavelength range of visible light. Hence, the resolution of SEM can be much higher than that of an optical microscope. Surface analysis of the grown UTZC on a Joel JA 65 SEM showed a step-like structure on the surface of various proportions of UTZC which confirms the layer growth of UTZC. It is seen that the crystallite size increases due to compound formation and the samples are crack free with well-defined

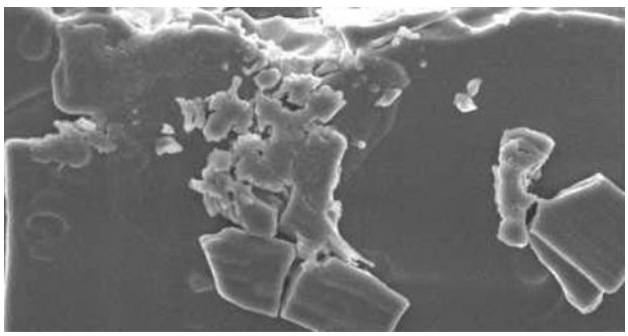

Fig. 10 SEM of 0.1UTZC

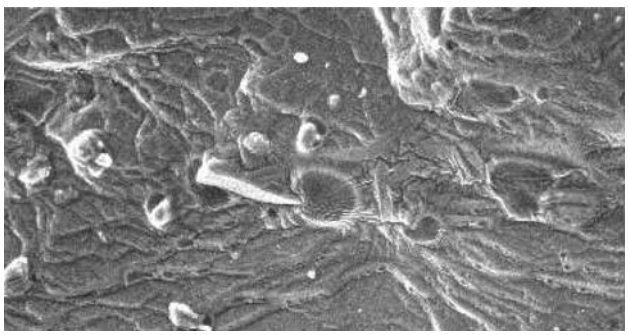

Fig. 11 SEM of 0.25UTZC

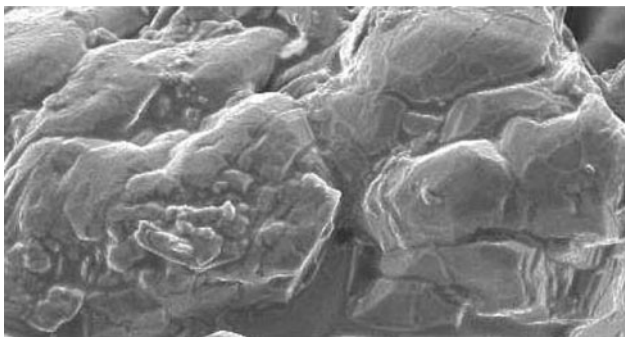

Fig. 12 SEM of 0.5UTZC

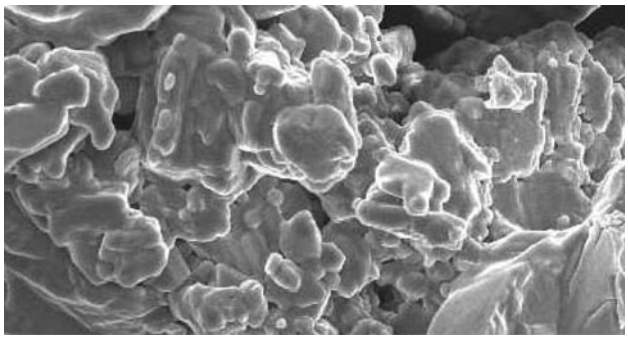

Fig. 13 SEM of 0.66UTZC

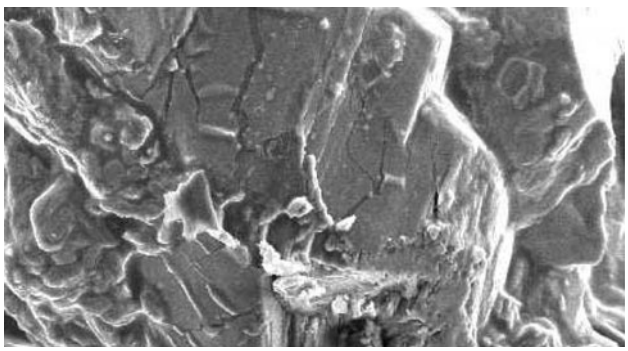

Fig. 14 SEM of 0.75UTZC

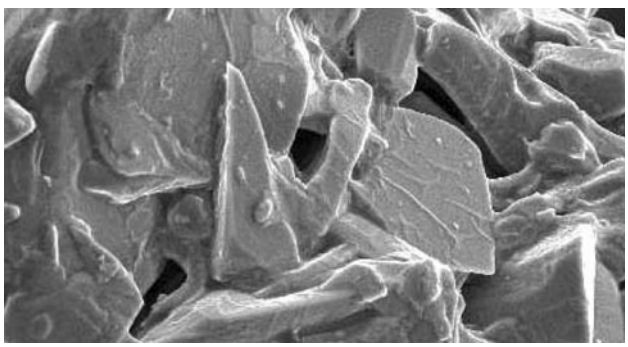

Fig. 15 SEM of 0.9UTZC

grain boundaries in various proportions of UTZC (Figs. 10, 11, 12, 13, 14 and 15).

Conclusions

(1) It was clearly shown from the Fig. 1 that the solubility decreases with increase in thiourea proportions.
(2) It was observed that for all the mixed crystals, the induction period decreased for 0.1 to 0.5UTZC and then slightly increased for 0.66 to 0.9UTZC.
(3) The interfacial tension can be calculated at various temperatures from the graph drawn between $\ln\tau$ and $1/(\ln S)^2$. The measured interfacial tensions vary from 2.82 to 4.54 mJ/m^2.
(4) The values of critical radius, number of molecules in the critical nucleus were decreased, and small values of free energy of activation in 0.5 proportion of urea–thiourea mixed crystal when compared to all other proportions predict the easy formation of nucleation in water.

References

1. Hall SR, Kolinsky PV, Jones R, Allen S, Gordon P, Bothwell B, Bloor D, Norman PA, Hursthouse M, Karaulov A, Baldwin J, Goodyear M, Bishop D. Polymorphism and nonlinear optical activity in organic crystals. J Cryst Growth. 1986;79:745–51.
2. Kurtz SK, Perry TT. A powder technique for the evaluation of nonlinear optical materials. J Appl Phys. 1968;39:3798–813.
3. Angelimary PA, Dhanuskodi S. Growth and characterization of a new nonlinear optic bisthiourea zinc chloride. Cryst Res Technol. 2001;36:1231–7.
4. Gupte SS, Desai CF. Vickers hardness anisotropy and slip system in zinc(tris)thioureasulphate crystals. Cryst Res Technol. 1999; 34:1329–32.
5. Zaitseva NP, Rashkovich LN, Bogatyreva SV. Stability of KH_2PO_4 and $K(H,D)_2PO_4$ solutions at fast crystal growth rates. J Cryst Growth. 1995;148:276–82.
6. Hameed SH, Ravi G, Dhanasekaran R, Ramasamy P. Growth and characterization of KDP and KAP. J Cryst Growth. 2000;212: 227–34.
7. Boomadevi S, Dhanasekaran R, Ramasamy P. Investigation on nucleation kinetics of urea crystals from methanol. Cryst Res Technol. 2002;37:159–68.
8. Sangwal K, Mielniczek-Brzoska E. Effect of impurities on metastable zone width for the growth of ammonium oxalate monohydrate crystals from aqueous solutions. J Cryst Growth. 2004;267:662–75.
9. Krishnan H, Justin C, Jerome S. Growth and characterization of novel ferroelectric urea-succinic acid single crystals. J Cryst Growth. 2008;310:3313–7.
10. Ushasree PM, Jayavel R, Ramasamy P. Growth and characterization of phosphate mixed ZTS single crystals. Mater Sci Eng B. 1999;65:153–8.
11. Skorsepa JS, Gyoryova K, Melnik M. Preparation, identification and thermal properties of $(CH_3CH_2COO)_2Zn{\cdot}2L{\cdot}H_2O$ ($-L =$ thiourea, nicotinamide, caffeine or theorbromine). J Therm Anal. 1995;44:169–77.
12. Rajasekaran R, Rajendran KV. Investigation on nucleation of cadmium thiourea chloride single crystals. Mater Chem Phys. 2003;82:273–80.
13. Verma S, Singh MK, Wadhavan VK, Suresh CH. Growth morphology of zinctris(thiourea)sulphate crystals. J Phys. 2000;54: 879–84.
14. Nyvlt J, Rychly R, Gottfried J, Wurzelova J. Metastable zone-width of bismuth thiourea bromide aqueous solutions. J Cryst Growth. 1970;6:151–62.
15. Madhurambal G, Mojumdar SC, Hariharan S, Ramasamy P. TG, DTC, FT-IR and Raman spectral analysis of Zn_a/Mg_b ammonium sulfate mixed crystals. J Therm Anal Calorim. 2004;78:125–33.
16. Czakis-Sulikowska D, Czylkowska A, Malinowska A. Thermal and other properties of new 4,4′-bipyridinetrichloroacetato complexes of Mn(II), Ni(II) and Zn(II). J Therm Anal Calorim. 2002;67:667–78.
17. More A, Verenkar VMS, Mojumdar SC. Nickel ferrite nanoparticles synthesis from novel fumarato-hydrazinate precursor. J Therm Anal Calorim. 2008;94:63–7.
18. Mojumdar SC, Raki L. Preparation, thermal, spectral and microscopic studies of calcium silicate hydrate-poly(acrylic acid) nanocomposite materials. J Therm Anal Calorim. 2006;85:99–105.
19. Sawant SY, Verenkar VMS, Mojumdar SC. Preparation, thermal, XRD, chemical and FT-IR spectral analysis of $NiMn_2O_4$ nanoparticles and respective precursor. J Therm Anal Calorim. 2007; 90:669–72.
20. Porob RA, Khan SZ, Mojumdar SC, Verenkar VMS. Synthesis, TG, SDC and infrared spectral study of $NiMn_2(C_4H_4O_4)_3{\cdot}6N_2H_4$—a precursor for $NiMn_2O_4$ nanoparticles. J Therm Anal Calorim. 2006;86:605–8.
21. Mojumdar SC, Varshney KG, Agrawal A. Hybrid fibrous ion exchange materials: past, present and future. Res J Chem Environ. 2006;10:89–103.
22. Doval M, Palou M, Mojumdar SC. Hydration behaviour of C_2S and C_2AS nanomaterials, synthesized by sol-gel method. J Therm Anal Calorim. 2006;86:595–9.
23. Varshney KG, Agrawal A, Mojumdar SC. Pyridine based thorium(IV) phosphate hybrid fibrous ion exchanger: synthesis, characterization and thermal behaviour. J Therm Anal Calorim. 2007;90:721–4.
24. Madhurambal G, Ramasamy P, Anbusrinivasan P, Mojumdar SC. Thermal properties, induction period, interfacial energy and nucleation parameters of solution grown benzophenone. J Therm Anal Calorim. 2007;90:673–9.
25. Varshney G, Agrawal A, Mojumdar SC. Pyridine based cerium(IV) phosphate hybrid fibrous ion exchanger: synthesis, characterization and thermal behaviour. J Therm Anal Calorim. 2007;90:731–4.
26. Mojumdar SC, Melnik M, Jona E. Thermal and spectral properties of Mg(II) and Cu(II) complexes with heterocyclic N-donor ligands. J Anal Appl Pyrolysis. 2000;53:149–60.
27. Borah B, Wood JL. Complex hydrogen bonded cations. The benzimidazole benzimidazolium cation. Can J Chem. 1976;50: 2470–81.
28. Mojumdar SC, Sain M, Prasad RC, Sun L, Venart JES. Selected thermoanalytical methods and their applications from medicine to construction. J Therm Anal Calorim. 2007;60:653–62.
29. Parthiban S, Murali S, Madhurambal G, Meenakshisundaram SP, Mojumdar SC. Effect of zinc(II) doping on thermal and optical properties of potassium hydrogen phthalate (KHP) crystals. J Therm Anal Calorim. 2010;100:751–6.